Mathematical Biosciences and Engineering

http://www.aimspress.com/journal/mbe

MBE, 20(4): 6666–6690.
DOI: 10.3934/mbe.2023287
Received: 25 November 2022
Revised: 05 January 2023
Accepted: 17 January 2023
Published: 03 February 2023

Research article

Analysis of Monkeypox viral infection with human to animal transmission via a fractional and Fractal-fractional operators with power law kernel

Alia M. Alzubaidi[1], Hakeem A. Othman[1], Saif Ullah[2,*], Nisar Ahmad[3] and Mohammad Mahtab Alam[4]

[1] Department of Mathematics, AL-Qunfudhah University college, Umm Al-Qura University, Saudi Arabia

[2] Department of Mathematics, University of Peshawar, Khyber Pakhtunkhwa, Pakistan

[3] Institute of Numerical Sciences Kohat University of Science and Technology (KUST) Kohat, Pakistan.

[4] Department of Basic Medical Sciences, College of Applied Medical Science, King Khalid University, Abha 61421, Saudi Arabia

* **Correspondence:** Email: saifullah.maths@uop.edu.pk.

Abstract: Monkeypox (MPX) is a global public health concern. This infectious disease affects people all over the world, not just those in West and Central Africa. Various approaches have been used to study epidemiology, the source of infection, and patterns of transmission of MPX. In this article, we analyze the dynamics of MPX using a fractional mathematical model with a power law kernel. The human-to-animal transmission is considered in the model formulation. The fractional model is further reformulated via a generalized fractal-fractional differential operator in the Caputo sense. The basic mathematical including the existence and uniqueness of both fractional and fractal-fractional problems are provided using fixed points theorems. A numerical scheme for the proposed model is obtained using an efficient iterative method. Moreover, detailed simulation results are shown for different fractional orders in the first stage. Finally, a number of graphical results of fractal-fractional MPX transmission models are presented showing the combined effect of fractal and fractional orders on model dynamics. The resulting simulations conclude that the new fractal-fractional operator added more biological insight into the dynamics of illness.

Keywords: Monkeypox mathematical model; fractal-fractional Caputo operator; existence and uniqueness; numerical results

1. Introduction

Monkeypox is a viral zoonotic disease caused by the monkeypox virus. This infection primarily occurs in Central and West Africa. MPX emerged as a serious orthopoxvirus for human health in 1980, when smallpox infection was eradicated. The first outbreak of this infection outside of African countries was reported in 2003 in the United States. Subsequently, many MPX-infected cases were reported in African and European countries. In May 2022, the infection was confirmed in several non-endemic areas. More than 3413 confirmed cases were reported with 1 death case to WHO from 50 countries/territories. The transmission of MPX occurs from animals to humans. Mostly, the hosts in animals include a range of rodents and non-human primates. The infection can also be spread from person to person through close contact, such as droplets released by talking, breathing, or sneezing. It can also be transmitted through sexual contact with an infectious person. Environmental transmission is also possible for MPX. In a recent investigation, the transmission of MPX from infected humans to pets are reported [1, 2]. Different disease symptoms are observed in MPX-infected people. Some people have less severe symptoms, while others develop more serious illnesses. Typical clinical symptoms developed by infected individuals during recent outbreaks include headache, fever, back pain, myalgia, lack of energy, swollen lymph nodes, and a rash lasting 2–3 weeks. Initially, a vaccine used against the smallpox eradication program protects her MPX. Three vaccines against MPX are currently available. Two of them, namely MVA-BN and LC16, have been approved to prevent this infection [1–3].

Many epidemiological aspects of MPX infection are still under investigation. Studies are underway to find out more about the transmission and treatment of this infection. Mathematical models are one of the most effective tools for studying the dynamic aspects of infectious diseases. These models help design effective interventions and provide decision-makers and the health sector with useful information for understanding disease dynamics and control. In this regard, a number of epidemiological infection models based on various infectious diseases have been developed and studied in the recent literature. These models are usually formulated using various differential derivatives (or operators), usually partial, stochastic, ordinary or fractional in nature [4–6]. The impact of treatment and vaccination on the dynamics of MPX is analyzed through a classical integer case transmission model in [7]. Recently, a new mathematical model-based MPX transmission is proposed in [8]. The authors of [8] divided the population into human and non-human (animal) classes and performed a detailed theoretical and numerical analysis of the problem. A mathematical model for the transmission of HIV and MPX co-infection is analyzed in [9]. The authors in [9] analyzed the transmission in the HIV-infected population and suggested some effective control interventions for disease eradication. In [10], the authors recently reviewed a stochastic MPX transmission model with cross-infection. Most of the existing MPX transmission models are established through classical integer-order differential equations. However, from an epidemiological point of view, Prior experience and history of an epidemic have a substantial role in analyzing the disease dynamics in a quite realistic way. On the other hand, the models with classical derivatives are local in nature and cannot model the dynamics of phenomena between two integer values. Furthermore, these classical models are unable to possess memory effects and hereditary properties which are found in many biological diseases. Subsequently, fractional operators have been used in recent years to formulate the biological models. The well-known operators having fractional order used in the existing literature are Caputo [11], Caputo-Fabrizio (CF) [12] and the Atangana-Baleanu operators(ABC) [13]. So far, only a few transmission models have been

established with these operators. A fractional-order MPX transmission model was recently developed in [14]. The authors of [14] formulated the model via the CF operator and estimated the parameters using real data reported in Nigeria over a specific time period. Furthermore, a fractional Caputo-type MPX transmission model is established in [15].

Besides the above-cited literature, the modeling approach with a novel fractal-fractional operator was adopted after the introduction of these operators by Atangana in 2017 [16]. These novel operators are actually the combination of fractional and fractal calculus. Recently, many researchers have applied these new concepts successfully in various scientific problems including epidemiology. For instance, a compartmental model to study the impact of commercial and rural banks via a fractional-fractal modeling approach [17]. They have shown that by using a model with the fractional-fractal operator one can provide a better fit to actual data. An application of fractional-fractal operators to analyze the dynamics of the novel coronavirus pandemic can be found in [18].

In existing literate, MPX transmission models are formulated with only animal-to-human transmission. Recently, transmission from humans to pets is being reported [2]. Based on the recent facts, in this paper, we develop the MPX transmission model with animal-to-human and human-to-animal transmission of infection. The proposed model is actually the extension of [10] by incorporating the human-to-animal transmission. In addition, unlike the existing models, we formulate the present problem using the fractional and fractal-fractional operators in order to gain more insights into the disease dynamics. The paper is classified into seven main sections with details as: Basic definition of the fractional, as well as the fractal-fractional operators are discussed in Section 2. Section 3 briefly introduces the model formulation for the integer case. The fractional MPX transmission model with some of the basic analysis is established in Section 4. Section 5 presents the numerical scheme and resulting simulation in the fractional MPX transmission model. The MPX model in fractal-fractional the case is developed in Section 6. Moreover, this section includes the existence, uniqueness, and novel numerical procedure along with simulation results and a brief discussion of the MPX model with the fractal-fractional operator. Finally, concluding remarks are drawn in Section 7.

2. Basic definitions

This section provides basic details about fractional and fractal-fractional operators developed [11, 16].

Definition 2.1. *Consider the function $\mathbf{X}(t) \in C^n$, the Caputo derivative with $n-1 < \rho \leq n$ as fractional order and $n \in \mathbb{N}$ is given as:*

$$ {}^{C}D_t^{\rho}(\mathbf{X}(t)) = \frac{1}{\Gamma(n-\rho)} \int_0^t \frac{\mathbf{X}^n(\zeta)}{(t-\zeta)^{\rho-n+1}} d\zeta. $$

${}^{C}D_t^{\rho}(\mathbf{X}(t))$ approaches to integer derivative as $\rho \to 1$.

Definition 2.2. *A point x^* is said to be the equilibrium point of the following Caputo-type system defined by:*

$$ {}^{C}D_t^{\rho} x(t) = f(t, x(t)), \quad \rho \in (0, 1), \tag{2.1} $$

if and only if $f(t, x^*) = 0$.

Let $\mathbb{X}(t)$ be continuously fractal differentiable function on (a_1, a_2). The fractal and fractional parameters are respectively η and ρ. We recalled some definitions as follows [16]:

Definition 2.3. *The fractal-fractional (FF) operator of the Riemann-Liouville (RL) type based on the power-law kernel is defined as:*

$$^{FF-P}D_{0,t}^{\rho,\eta}\Big(\mathbb{X}(t)\Big) = \frac{1}{\Gamma(n-\rho)}\frac{d}{dt^{\eta}}\int_0^t (t-\zeta)^{n-\rho-1}\mathbb{X}(\zeta)d\zeta, \tag{2.2}$$

where, $n-1 < \rho, \eta \leq n \in \mathbb{N}$ *and* $\frac{d\mathbb{X}(\zeta)}{d\zeta^{\eta}} = \lim_{t\to\zeta}\frac{\mathbb{X}(t)-\mathbb{X}(\zeta)}{t^{\eta}-\zeta^{\eta}}$.

Definition 2.4. *The corresponding FF integral operator of (2.2) is given as follows:*

$$^{FF-P}J_{0,t}^{\rho}\Big(\mathbb{X}(t)\Big) = \frac{\eta}{\Gamma(\rho)}\int_0^t (t-\zeta)^{\rho-1}\zeta^{\eta-1}\mathbb{X}(\zeta)d\zeta. \tag{2.3}$$

3. Monkeypox model in integer case

This section briefly describes the proposed MPX transmission model. To develop the desired model, the whole human population is classified into four mutually-exclusive epidemiological classless including the susceptible human class $S_h(t)$, the infectious human class $I_h(t)$, isolate/quartine human class $Q_h(t)$ and the recovered human class $R_h(t)$. The non-human population (animals) is divided into two groups namely the susceptible animals $S_m(t)$ and the infectious animals $I_m(t)$. The considerable assumptions taken into account are:

- Unlike the existing models, we considered the transmission of infection to succeedable animals from infected humans.
- The disease-induced death rate is considered in infected and isolated compartments.
- The infectious human population can be recovered through proper treatment and natural recovery.

The susceptible human class is generated by a constant recruitment rate Λ_h and reduced by acquiring infection after interaction with infectious humans and animals. The force of infection is $\beta_1 I_m + \beta_2 I_h$, where β_1 and β_2 are the effective contact rates (capable of transmitting infection) corresponding to infectious animals and humans respectively. Each class containing the human population is reduced due to natural death at the rate μ. The Monkeypox-induced death rate in the infected and isolated human compartments are denoted by δ_1 and δ_2 respectively. The infectious human papulation becomes recovered and joins R_h at the rated r_1 and r_2. The symbol r_1 shows the natural recovery rate and r_2 denotes the recovery rate through specific treatment. The infectious human population is isolated and joins Q_h class at the transmission rate ϕ. The recovery rate of the isolated/quartine human population is denoted by τ_2 while τ_1 shows the susceptibility rate of the isolated population.

In the animal population, Λ_m shows the recruitment rate while the natural death rate denoted is ν. The force of infection is $\zeta_1 I_h + \zeta_2 I_m$, where ζ_1 and ζ_2 are the respective transmission rates corresponding to infected humans and animals.

Keeping the above discussion in mind the proposed MPX mathematical model is given in the fol-

lowing system.

$$\begin{aligned}
\frac{dS_h}{dt} &= \Lambda_h - \beta_1 S_h I_m - \beta_2 S_h I_h - \mu S_h + \tau_1 Q_h,\\
\frac{dI_h}{dt} &= \beta_1 S_h I_m + \beta_2 S_h I_h - (\mu + \delta_1 + \varphi + \mathtt{r}_1 + \mathtt{r}_2) I_h,\\
\frac{dQ_h}{dt} &= \varphi I_h - (\tau_1 + \tau_2 + \mu + \delta_2) Q_h,\\
\frac{dR_h}{dt} &= (\mathtt{r}_1 + \mathtt{r}_2) I_h + \tau_2 Q_h - \mu R_h,\\
\frac{dS_m}{dt} &= \Lambda_m - \zeta_1 S_m I_h - \zeta_2 S_m I_m - \nu S_m,\\
\frac{dI_m}{dt} &= \zeta_1 S_m I_h + \zeta_2 S_m I_m - \nu I_m.
\end{aligned} \tag{3.1}$$

The initial conditions for the above system are

$$\begin{aligned}
S_h(t_0) &= S_{h0} \geq 0, \quad I_h(t_0) = I_{h0} \geq 0, \quad Q_h(t_0) = Q_{h0} \geq 0, \quad R(t_0) = R_{h0} \geq 0,\\
S_m(t_0) &= S_{m0} \geq 0, \quad I_m(t_0) = I_{m0} \geq 0.
\end{aligned} \tag{3.2}$$

In order to make the onward calculation simpler, we take

$$\begin{aligned}
\lambda_h &= (\beta_1 I_m + \beta_2 I_h), \lambda_m = (\zeta_1 I_h + \zeta_2 I_m), \; k_1 = (\mu + \delta_1 + \varphi + \mathtt{r}_1 + \mathtt{r}_2),\\
k_2 &= (\tau_1 + \tau_2 + \mu + \delta_2).
\end{aligned}$$

Thus, the model (3.1) can be written as follows:

$$\begin{aligned}
\frac{dS_h(t)}{dt} &= \Lambda_h - \lambda_h S_h - \mu S_h + \tau_1 Q_h,\\
\frac{dI_h}{dt} &= \lambda_h S_h - k_1 I_h,\\
\frac{dQ_h}{dt} &= \varphi I_h - k_2 Q_h,\\
\frac{dR_h}{dt} &= (\mathtt{r}_1 + \mathtt{r}_2) I_h + \tau_2 Q_h - \mu R_h,\\
\frac{dS_m}{dt} &= \Lambda_m - \lambda_m S_m - \nu S_m,\\
\frac{dI_m}{dt} &= \lambda_m S_m - \nu I_m.
\end{aligned} \tag{3.3}$$

4. Fractional extension of MPX model

This section presents the extension of the integer MPX model to fractional order. The well-known Caputo operator with a power law kernel is utilized to obtain the fractional model. The transmission models establish with fractional operators provides biologically more significant output than integer case problems and have a widespread application in real-life situations including epidemiology. It is due to the memory and heredity properties of fractional operators. The procedure of developing fractional-order mathematical model we proceed as follows:

$$\begin{cases} \frac{dS_h}{dt} = \int_{t_0}^{t} k(t-t')[\Lambda_h - \lambda_h S_h - \mu S_h + \tau_1 Q_h]dt', \\ \frac{dI_h}{dt} = \int_{t_0}^{t} k(t-t')[\lambda_h S_h - k_1 I_h]dt', \\ \frac{dQ_h}{dt} = \int_{t_0}^{t} k(t-t')[\varphi I_h - k_2 Q_h]dt', \\ \frac{dR_h}{dt} = \int_{t_0}^{t} k(t-t')[(\mathtt{r}_1 + \mathtt{r}_2) I_h + \tau_2 Q_h - \mu R_h]dt', \\ \frac{dS_m}{dt} = \int_{t_0}^{t} k(t-t')[\Lambda_m - \lambda_m S_m - \nu S_m]dt', \\ \frac{dR_m}{dt} = \int_{t_0}^{t} k(t-t')[\lambda_m S_m - \nu I_m]dt'. \end{cases} \tag{4.1}$$

In the above problem $k(t-t')$ describes the time-dependent kernel. Moreover,

$$k(t-t') = \frac{(t-t')^{\rho-2}}{\Gamma(\rho-1)}, \tag{4.2}$$

Replacing (4.2) in (4.1), and taking the Caputo having order $\rho - 1$, it leads to

$$\begin{cases} {}^{C}D_t^{\rho-1}\left[\frac{dS_h}{dt}\right] &= {}^{C}D_t^{\rho-1} I_t^{-(\rho-1)}[\Lambda_h - \lambda_h S_h - \mu S_h + \tau_1 Q_h], \\ {}^{C}D_t^{\rho-1}\left[\frac{dI_h}{dt}\right] &= {}^{C}D_t^{\rho-1} I_t^{-(\rho-1)}[\lambda_h S_h - k_1 I_h], \\ {}^{C}D_t^{\rho-1}\left[\frac{dQ_h}{dt}\right] &= {}^{C}D_t^{\rho-1} I_t^{-(\rho-1)}[\varphi I_h - k_2 Q_h], \\ {}^{C}D_t^{\rho-1}\left[\frac{dR_h}{dt}\right] &= {}^{C}D_t^{\rho-1} I_t^{-(\rho-1)}[(\mathtt{r}_1 + \mathtt{r}_2) I_h + \tau_2 Q_h - \mu R_h], \\ {}^{C}D_t^{\rho-1}\left[\frac{dS_m}{dt}\right] &= {}^{C}D_t^{\rho-1} I_t^{-(\rho-1)}[\Lambda_m - \lambda_m S_m - \nu S_m], \\ {}^{C}D_t^{\rho-1}\left[\frac{dR_m}{dt}\right] &= {}^{C}D_t^{\rho-1} I_t^{-(\rho-1)}[\lambda_m S_m - \nu I_m]. \end{cases} \tag{4.3}$$

After some manipulation the fractional MPX transmission model leads to the following system

$$\begin{cases} {}^{C}D_t^{\rho} S_h &= \Lambda_h - \lambda_h S_h - \mu S_h + \tau_1 Q_h, \\ {}^{C}D_t^{\rho} I_h &= \lambda_h S_h - k_1 I_h, \\ {}^{C}D_t^{\rho} Q_h &= \varphi I_h - k_2 Q_h, \\ {}^{C}D_t^{\rho} R_h &= (\mathtt{r}_1 + \mathtt{r}_2) I_h + \tau_2 Q_h - \mu R_h, \\ {}^{C}D_t^{\rho} S_m &= \Lambda_m - \lambda_m S_m - \nu S_m \\ {}^{C}D_t^{\rho} I_m &= \lambda_m S_m - \nu I_m, \end{cases} \tag{4.4}$$

subject to ICs (3.2). In the system (4.4), ${}^{C}D_t^{\rho}$ shows the Caputo derivative with order $\rho \in (0, 1]$.

4.1. Basic analysis of the fractional MPX model

In this section we address some of the basic and necessary mathematical analysis of fractional MPX disease model.

4.1.1. Invariant region

The feasible domain in terms of biological point view for the MPX fractional model (4.4) is constructed as follows:

$$\begin{aligned} \Omega_h &= \left\{ (S_h, I_h, Q_h, R_h) \subset \mathbb{R}_+^4 : S_h + I_h + Q_h + R_h \leq \tfrac{\Lambda_h}{\mu} \right\}, \\ \Omega_m &= \left\{ (S_m, I_m) \subset \mathbb{R}_+^2 : S_m + I_m \leq \tfrac{\Lambda_m}{\nu} \right\}, \end{aligned} \tag{4.5}$$

Such that and we have $\Omega = \Omega_h \times \Omega_m \subset \mathbb{R}_+^4 \times \mathbb{R}_+^2$ is positively invariant.

The following theorem prove the positivity and bounded properties of solution of Caputo MPX model.

Theorem 4.1. *Let* $S_h(0) = S_{h_0}$, $I_h(0) = I_{h_0}$, $Q_h(0) = Q_{h_0}$, $R_h(0) = R_{h_0}$, $S_m(0) = S_{m_0}$, *and* $I_m(0) = I_{m_0}$ *be the initial values of state variables. For the positive initial conditions, the region defined in the set* Ω *will be positively invariant for all* $t > 0$. *Furthermore,* $N_{h_0}(t) \leq \frac{\Lambda_h}{\mu}$ *and* $N_{m_0}(t) \leq \frac{\Lambda_m}{\nu}$.

Proof. We start the proof by considering only the first equation of system (4.4). Let S_{h_0}, I_{h_0}, Q_{h_0}, R_{h_0}, S_{m_0} *and* I_{m_0}, be all positive, the desired result is to prove that state variables are positive. From system (4.4) we have

$${}^{C}D_t^{\rho} S_h = \Lambda_h - \lambda_h S_h - \mu S_h + \tau_1 Q_h, \tag{4.6}$$

then

$${}^{C}D_t^{\rho} S_h + (\lambda_h + \mu) S_h = \Lambda_h + \tau_1 Q_h. \tag{4.7}$$

Since $\Lambda_h + \tau_1 Q_h \geq 0$ implies that ${}^C D_t^\rho S_h + (\lambda_h + \mu) S_h \geq 0$, by using the Laplace transform we have

$$\begin{aligned} &L\left[{}^C D_t^\rho S_h\right] + L\left[(\lambda_h + \mu) S_h\right] \geq 0, \\ &s^\rho S_h(s) - s^{\rho-1} S_h(0) + (\lambda_h + \mu) S_h(s) \geq 0, \\ &S_h(s) \geq \frac{s^{\rho-1}}{(s^\rho + (\lambda_h + \mu))} S_{h_0}. \end{aligned}$$

By applying the inverse Laplace transform we have

$$S_h(t) \geq E_{\rho,1}\left(-(\lambda_h + \mu) t^\rho\right) S_{h_0}. \tag{4.8}$$

Since quantities on right hand side of (4.8) are positive therefore, we have $S_h \geq 0$ for $t \geq 0$. Similarly, it can be shown that $I_h, Q_h, R_h, S_m,$ *and* $I_m \geq 0 \ \ \forall t \geq 0$. Thus, the solutions in $\mathbb{R}_+^4 \times \mathbb{R}_+^2$ are positive.

In the second part, we prove the bounded property of the problem solution. The total population for human is given by $N_h(t) = S_h(t) + I_h(t) + Q_h(t) + R_h(t)$, Such that

$${}^C D_t^\rho N_h(t) = {}^C D_t^\rho S_h(t) + {}^C D_t^\rho I_h(t) + {}^C D_t^\rho Q_h(t) + {}^C D_t^\rho R_h(t). \tag{4.9}$$

$$\begin{aligned} &{}^C D_t^\rho N_h(t) = \Lambda_h - (\delta_1 I_h + \delta_2 Q_h) - \mu N_h(t) \leq \Lambda_h - \mu N_h(t), \\ &{}^C D_t^\rho N_h(t) \leq \Lambda_h - \mu N_h(t), \end{aligned}$$

Laplace transform on both sides yields to the following

$$L\left[{}^C D_t^\rho N_h(t)\right] \leq L\left[\Lambda_h - \mu N_h(t)\right],$$

$$s^\rho N_h(s) - s^{\rho-1} N_h(0) + \mu N_h(s) \leq \tfrac{\Lambda_h}{s},$$

$$N_h(s) \leq \tfrac{s^{\rho-1}}{(s^\rho+\mu)} N_h(0) + \tfrac{\Lambda_h}{s(s^\rho+\mu)}.$$

By applying inverse Laplace transform we have

$$N_h(t) \leq E_{\rho,1}\left(-\mu t^\rho\right) N_h(0) + \Lambda_h E_{\rho,\rho+1}\left(-\mu t^\rho\right). \tag{4.10}$$

By taking limit $t \to \infty$ we have implies that $N_h(t) \leq \frac{\Lambda_h}{\mu}$, If $N_{h_0}(t) \leq \frac{\Lambda_h}{\mu}$ *then* $N_h(t) \leq \frac{\Lambda_h}{\mu}$ implies $N_h(t)$ is bounded. In similar way we can prove that $N_m(t)$ is bounded. So we conclude that the region Ω is epidemiological feasible and bounded.

4.2. Equilibria and $\mathcal{R}_0$

For equilibrium points, we consider the following system

$$\begin{cases} {}^C D_t^\rho S_h = & 0, \\ {}^C D_t^\rho I_h = & 0, \\ {}^C D_t^\rho Q_h = & 0, \\ {}^C D_t^\rho R_h = & 0, \\ {}^C D_t^\rho S_m = & 0, \\ {}^C D_t^\rho I_m = & 0. \end{cases} \tag{4.11}$$

The solution of (4.11) at disease free state (i.e., $I_h = Q_h = R_h = I_m = 0$) gives the following disease free equilibrium (DFE).

$$E^0 = (S_h^0, I_h^0, Q_h^0, R_h^0, S_m^0, I_m^0) = \left(\frac{\Lambda_h}{\mu}, 0, 0, 0, \frac{\Lambda_m}{\nu}, 0\right),$$

By using the next generation method we compute $\mathcal{R}_0$.
Let $X = (I_h, Q_h, I_m)^t$ then have Jacobian of the linearized system at DFE is as follows

$$\mathcal{F} = \begin{pmatrix} \frac{\beta_2\Lambda_h}{\mu} & 0 & \frac{\beta_1\Lambda_h}{\mu} \\ 0 & 0 & 0 \\ \frac{\zeta_1\Lambda_m}{\nu} & 0 & \frac{\zeta_2\Lambda_m}{\nu} \end{pmatrix}, \ \mathcal{V} = \begin{pmatrix} k_1 & 0 & 0 \\ -\varphi & k_2 & 0 \\ 0 & 0 & \nu \end{pmatrix}, \tag{4.12}$$

The next generation matrix is given by

$$\mathbf{FV}^{-1} = \begin{pmatrix} \frac{\beta_2\Lambda_h}{\mu k_1} & 0 & \frac{\beta_1\Lambda_h}{\mu\nu} \\ 0 & 0 & 0 \\ \frac{\zeta_1\Lambda_m}{\nu k_1} & 0 & \frac{\zeta_2\Lambda_m}{\nu^2} \end{pmatrix}, \tag{4.13}$$

$$\mathcal{R}_0 = (\mathcal{R}_1 + \mathcal{R}_2) = \frac{1}{2}\left(\frac{\left(\nu\beta_2 S_h^0 + \varsigma_2 k_1 S_m^0\right)}{\nu k_1} + \frac{\left(\nu\beta_2 S_h^0 + \varsigma_2 k_1 S_m^0\right)}{\nu k_1}\sqrt{1 + \frac{4\nu k_1 S_m^0 S_h^0(\beta_1\zeta_1 - \beta_2\zeta_2)}{\left(\nu\beta_2 S_h^0 + \varsigma_2 k_1 S_m^0\right)^2}}\right).$$

Endemic equilibrium point The endemic equilibrium (EE) of the fractional MPX infection model is obtain as follows:

$$\begin{aligned} S_h^* &= \tfrac{k_1 k_2 \Lambda_h}{\mu k_1 k_2 + (k_1 k_2 - \phi\tau_1)\lambda_h^*}, \\ I_h^* &= \tfrac{\lambda_h^* S_h^*}{k_1}, \\ Q_h^* &= \tfrac{\phi\lambda_h^* S_h^*}{k_1 k_2}, \\ R_h^* &= \tfrac{(r_1+r_2)\lambda_h^* S_h^*}{\mu k_1} + \tfrac{\phi\lambda_h^*\tau_2 S_h^*}{\mu k_1 k_2}, \\ S_m^* &= \tfrac{\Lambda_m}{\nu+\lambda_m^*}, \\ I_m^* &= \tfrac{\lambda_m^* S_m^*}{\nu}. \end{aligned} \tag{4.14}$$

5. Numerical treatment of fractional MPX model

In this section, the iterative solution of the MPX model (4.4) in fractional case is being investigated. Moreover, the resulting simulation will be analyzed in detail.

5.1. Numerical scheme

The fractional Euler's scheme as discussed in the recent literature [19, 20] is utilized to obtain numerical scheme of the proposed model. For this purpose, we express the fractional model (4.4) in the following problem

$$\begin{cases} {}^{C}D_t^{\rho} p(t) = \mathcal{H}(t, p(t)), \\ p(0) = p_0, \quad 0 < \mathcal{T} < \infty, \end{cases} \tag{5.1}$$

where, $p(t) = (S_h, I_h, Q_h, R_h, S_m, I_m) \in \mathbb{R}^6$ and p_0 stands for initial state vector. Further, $\mathcal{H}(t, p(t)) = (\mathcal{H}_1(t, p(t)), \mathcal{H}_2(t, p(t)), \mathcal{H}_3(t, p(t)), \mathcal{H}_4(t, p(t)), \mathcal{H}_5(t, p(t)), \mathcal{H}_6(t, p(t)))$ denotes continuous real valued vector function satisfying the Lipschitz condition such that

$$\begin{cases} \mathcal{H}_1(t, p(t)) = \Lambda_h - \lambda_h S_h - \mu S_h + \tau_1 Q_h, \\ \mathcal{H}_2(t, p(t)) = \lambda_h S_h - k_1 I_h, \\ \mathcal{H}_3(t, p(t)) = \varphi I_h - k_2 Q_h, \\ \mathcal{H}_4(t, p(t)) = (\mathtt{r}_1 + \mathtt{r}_2) I_h + \tau_2 Q_h - \mu R_h, \\ \mathcal{H}_5(t, p(t)) = \Lambda_m - \lambda_m S_m - \nu S_m, \\ \mathcal{H}_6(t, p(t)) = \lambda_m S_m - \nu I_m. \end{cases} \tag{5.2}$$

Taking the Caputo integral on both sides of (5.1) we obtained

$$p(t) = p_0 + \frac{1}{\Gamma(\rho)} \int_0^t (t - \varsigma)^{\rho - 1} \mathcal{H}(\varsigma, p(\varsigma)) d\varsigma. \tag{5.3}$$

Further, a uniform grid on the interval $[0, \mathcal{T}]$, with $\mathfrak{h} = \frac{\mathcal{T}-0}{m}$, denotes the step size and $m \in \mathbb{N}$ is considered. Using the Euler method [20], the Eq (5.3) leads to the following result:

$$\begin{cases} p_{n+1} = p_0 + \frac{\mathfrak{h}^{\rho}}{\Gamma(\rho+1)} \sum_{\iota=0}^{n} ((n - \iota + 1)^{\rho} - (n - \iota)^{\rho}) \mathcal{H}(t_\iota, p(t_\iota)), \\ n = 0, , \cdots, m. \end{cases} \tag{5.4}$$

Utilizing the numerical procedure (5.4) and the expressions in (5.2), the following iterative formulae are establish for MPX transmission model (4.4):

$$\begin{aligned} S_{hn+1} &= S_{h0} + \frac{\mathfrak{h}^{\rho}}{\Gamma(\rho + 1)} \sum_{\iota=0}^{n} ((n - \iota + 1)^{\rho} - (n - \iota)^{\rho}) \Big(\Lambda_h - \lambda_{h\iota} S_{h\iota} - \mu S_{h\iota} + \tau_1 Q_{h\iota} \Big), \\ I_{hn+1} &= I_{h0} + \frac{\mathfrak{h}^{\rho}}{\Gamma(\rho + 1)} \sum_{\iota=0}^{n} ((n - \iota + 1)^{\rho} - (n - \iota)^{\rho}) \Big(\lambda_{h\iota} S_{h\iota} - k_1 I_{h\iota} \Big), \\ Q_{hn+1} &= Q_{h0} + \frac{\mathfrak{h}^{\rho}}{\Gamma(\rho + 1)} \sum_{\iota=0}^{n} ((n - \iota + 1)^{\rho} - (n - \iota)^{\rho}) \Big(\varphi I_{h\iota} - k_2 Q_{h\iota} \Big), \end{aligned}$$

$$
\begin{aligned}
R_{hn+1} &= R_{h0} + \frac{\mathbb{h}^{\rho}}{\Gamma(\rho+1)} \sum_{\iota=0}^{n} ((n-\iota+1)^{\rho} - (n-\iota)^{\rho}) \Big((\mathtt{r}_1 + \mathtt{r}_2) I_{h\iota} + \tau_2 Q_{h\iota} - \mu R_{h\iota} \Big), \\
S_{mn+1} &= S_{m0} + \frac{\mathbb{h}^{\rho}}{\Gamma(\rho+1)} \sum_{\iota=0}^{n} ((n-\iota+1)^{\rho} - (n-\iota)^{\rho}) \Big(\Lambda_m - \lambda_{m\iota} S_{m\iota} - \nu S_{m\iota} \Big), \\
I_{mn+1} &= I_{m0} + \frac{\mathbb{h}^{\rho}}{\Gamma(\rho+1)} \sum_{\iota=0}^{n} ((n-\iota+1)^{\rho} - (n-\iota)^{\rho}) \Big(\lambda_m \nu S_{m\iota} - \nu I_{m\iota} \Big). \qquad (5.5)
\end{aligned}
$$

5.2. Simulation

In this section, we simulate the fractional case MPX infection model (4.4) using the iterative scheme derived in Eq (5.5). The time level considered in the graphical results of the model is 500 days. The model is simulated for two sets of variables and five different values of fractional order ρ. The values of parameters are taken from [10].

Case 1: In this case, we consider the parameters values as $\Lambda_h = 10$, $\beta_1 = 0.00001$, $\beta_2 = 0.00002$, $\mu = 0.05$, $\delta = 0.0003$, $\tau_1 = 0.32$, $\tau_2 = 0.2; \varphi = 0.5$, $r_1 = 0.041$, $r_2 = 0.043$, $\alpha_1 = 0.004$, $\delta_2 = 0.002$, $\Lambda_m = 10$, $\zeta_1 = 0.000027$, $\zeta_2 = 0.000017$, $\nu = 0.02$. The graphical interpretation for this case is shown in Figure 1(a)–(f). The dynamics of susceptible, infected, isolated and recovered human population are depicted in Figure 1(a)–(d) respectively. The dynamics of susceptible and infected animals population is shown in Figure 1(e),(f) respectively. These graphical interpretations demonstrated that all solution trajectories converge to the DFE for all values of ρ.

Case 2: In this case, we slightly modify the parameters values. The considered parameters values are $\Lambda_h = 10$, $\beta_1 = 0.0001$, $\beta_2 = 0.0002$, $\mu = 0.05$, $\delta = 0.0003$, $\tau_1 = 0.32$, $\tau_2 = 0.2; \varphi = 0.5$, $r_1 = 0.041$, $r_2 = 0.043$, $\alpha_1 = 0.004$, $\delta_2 = 0.002$, $\Lambda_m = 10$, $\zeta_1 = 0.00027$, $\zeta_2 = 0.00017$, $\nu = 0.02$. The graphical results, in this case, are depicted in Figure 2(a)–(f). In Figure 2(a)–(d), we have shown the dynamics of the susceptible, infected, isolated, and recovered human population respectively, while in Figure 2(e),(f) describes the dynamics of susceptible and infected animals population respectively. These simulations demonstrated that all solution trajectories converge to the EE for all values of ρ.

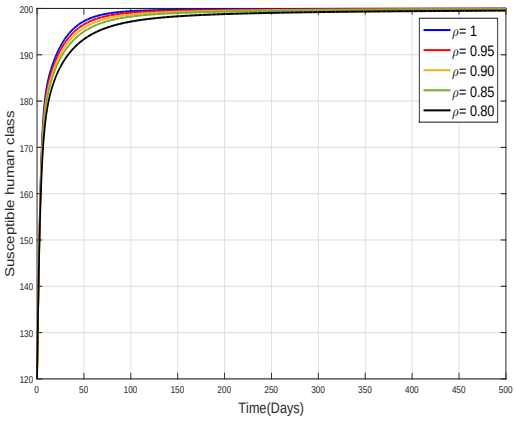

(a)

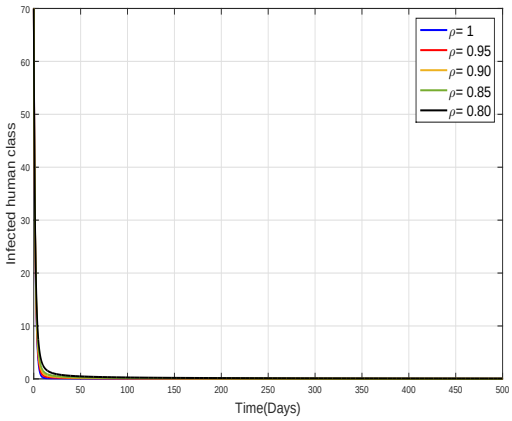

(b)

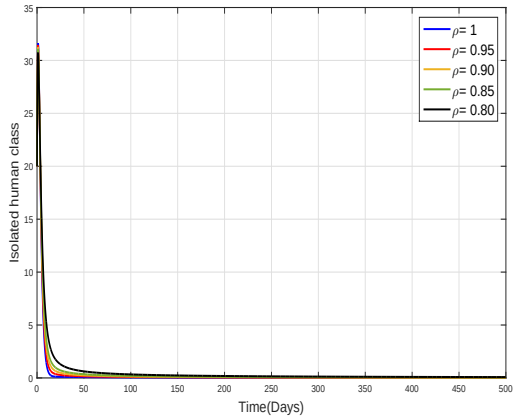

(c)

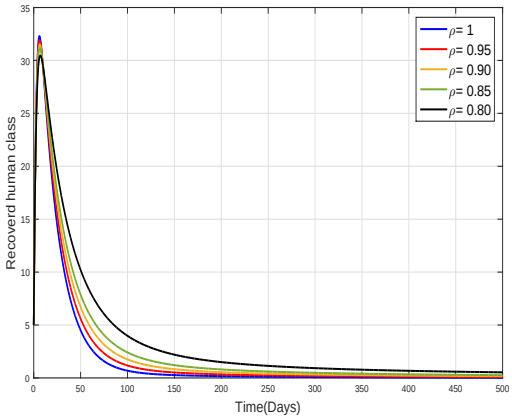

(d)

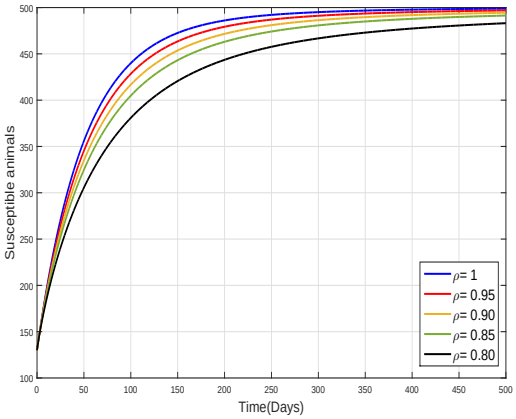

(e)

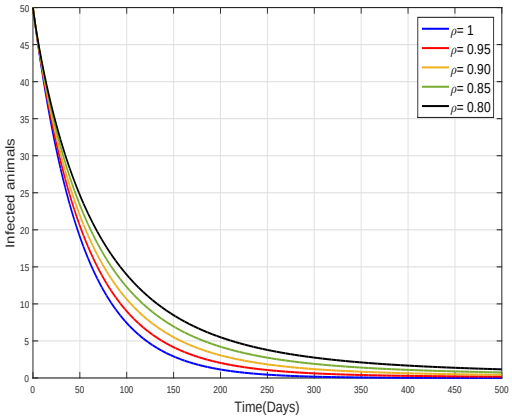

(f)

Figure 1. Dynamics of the Caputo MPX transmission model (4.4) for different values of fractional order $\rho = 1, 0.95, 0.90, 0.85, 0.80$. The parameters values given in case 1 are considered for simulation.

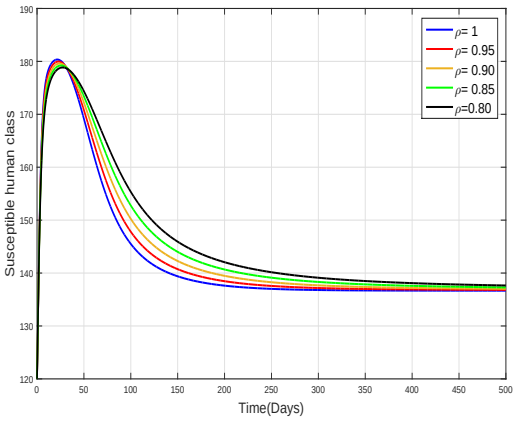

(a)

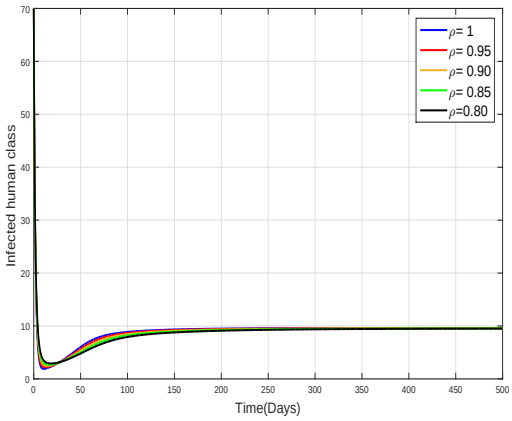

(b)

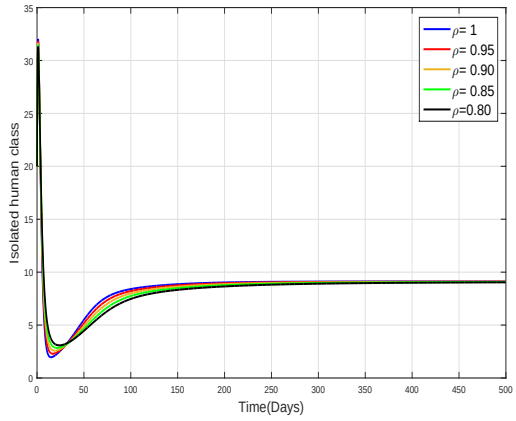

(c)

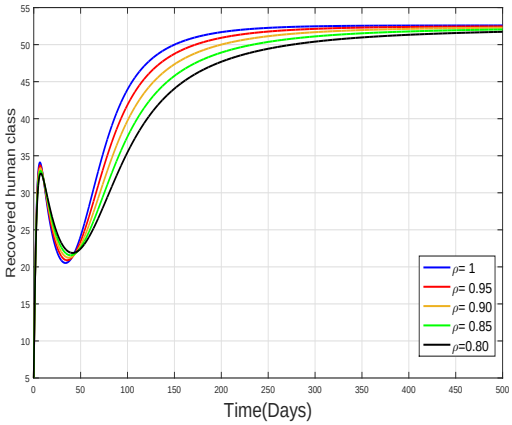

(d)

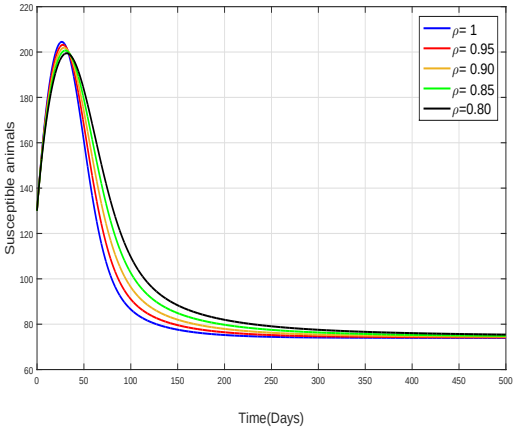

(e)

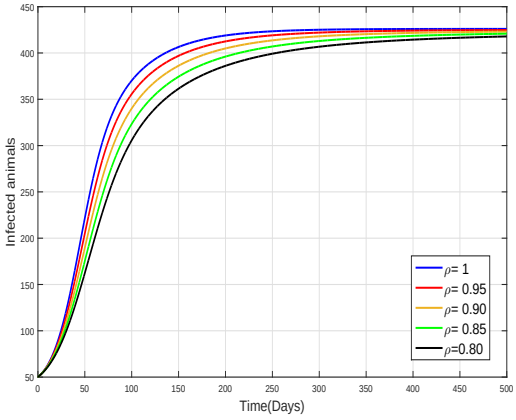

(f)

Figure 2. Dynamics of the Caputo MPX transmission model (4.4) for different values of fractional order $\rho = 1, 0.95, 0.90, 0.85, 0.80$ by considering parameter values given in case 2.

6. A fractal-fractional MPX model in Caputo sense

In the previous section, we extended the integer MPX transmission model to a fractional case. In this part of the manuscript, we further extend the fractional model to obtain a more generalized problem using the fractal-fractional operator in the Caputo sense. After formulating the model, we explore its basic mathematical analysis including the existence and uniqueness of the solution. Moreover, the model in the fractal-fractional case will be solved via an efficient numerical scheme to simulate the model for different values of fractional as well as fractal orders. The fractal-fractional case MPX transmission model can be established by the following system

$$\begin{aligned}
{}^{FF}D_{0,t}^{\rho,\eta}\Big(S_h(t)\Big) &= \Lambda_h - \lambda_h S_h - \mu S_h + \tau_1 Q_h,\\
{}^{FF}D_{0,t}^{\rho,\eta}\Big(I_h(t)\Big) &= \lambda_h S_h - k_1 I_h,\\
{}^{FF}D_{0,t}^{\rho,\eta}\Big(Q_h(t)\Big) &= \varphi I_h - k_2 Q_h,\\
{}^{FF}D_{0,t}^{\rho,\eta}\Big(R_h(t)\Big) &= (\mathtt{r}_1 + \mathtt{r}_2) I_h + \tau_2 Q_h - \mu R_h,\\
{}^{FF}D_{0,t}^{\rho,\eta}\Big(S_m(t)\Big) &= \Lambda_m - \lambda_m S_m - \nu S_m,\\
{}^{FF}D_{0,t}^{\rho,\eta}\Big(I_m(t)\Big) &= \lambda_m S_m - \nu I_m.
\end{aligned} \tag{6.1}$$

The fractional and fractal parameters in the above model (6.1) are expressed by ρ and η respectively. We proceed with the basic analysis of the model (6.1) in the next section.

6.1. Existence and uniqueness

The current part of the work explores the existence of the uniqueness of the proposed model solution using the well-known Picard-Lindelöf theorem coupled with the fixed point approach. To move further, the fractal-fractional system (6.1) can be expressed in the following general Cauchy problem

$$\begin{cases} {}^{FF}D_{0,t}^{\rho,\eta} p(t) = \mathcal{H}(t, p(t)),\\ p(0) = p_0, \quad 0 < t < \mathcal{T} < \infty, \end{cases} \tag{6.2}$$

where, $p(t) = (S_h, I_h, Q_h, R_h, S_m, I_m)$ consists of state variables and $\mathcal{H}$ representing a continuous vector function as described in Subsection 5.1. The corresponding initial condition are stated as $p_0 = (S_h(0), I_h(0), Q_h(0), R_h(0), S_m(0), I_m(0))$.

The problem (6.2) leads to the following result after utilizing the fractional integral

$$\frac{1}{\Gamma(1-\rho)}\frac{d}{dt}\int_0^t (t-\varsigma)^{-\rho}\mathcal{H}(t, p(t))d\varsigma = \eta t^{\eta-1}\mathcal{H}(t, p(t)). \tag{6.3}$$

After the replacement of right hand side by the Caputo derivative and then implementing the integral we obtain [21]:

$$p(t) = p(0) + \frac{\eta}{\Gamma(\rho)}\int_0^t (t-\varsigma)^{\rho-1}\varsigma^{\eta-1}\mathcal{H}(\varsigma, g(\varsigma))d\varsigma. \tag{6.4}$$

Further, with the help of Picard-Lindelöf theorem, let we define

$$\prod_{a}^{b} = \mathbb{I}_n(t_n) \times \overline{\mathbb{A}_0(p_0)},$$

where,

$$\mathbb{I}_n(t_n) = [t_{n-a}, t_{a+n}],\ \overline{\mathbb{A}_0(p_0)} = [t_0 + b, b + t_0].$$

Defining the following operator

$$\Lambda.C[\mathbb{I}_n(t_n), \mathbb{A}_b(t_n)] \to C(\mathbb{I}_n(t_n), \mathbb{A}_b(t_n)),$$

such that

$$\Lambda\phi(t) = p(0) + \frac{\eta}{\Gamma(\rho)} \int_0^t (t - \varsigma)^{\rho-1} \varsigma^{\eta-1} \mathcal{H}(\varsigma, \phi(\varsigma)) d\varsigma. \tag{6.5}$$

Our focus is to confirm the fact that operator defined in (6.5) maps a complete norm empty metric space into itself. Moreover, it is necessary to establish that it also possesses the contraction mapping. In the first attempt we show that

$$\|\Lambda\phi(t) - p(0)\| \leq c. \tag{6.6}$$

The following norm is taken into account

$$\begin{aligned} \|\Lambda\phi(t) - p(0)\| &\leq \frac{\eta}{\Gamma(\rho)} \int_0^t (t - \varsigma)^{\rho} \varsigma^{\eta-1} \|\mathcal{H}(\varsigma, p(\varsigma))\|_\infty d\varsigma \\ &\leq \frac{\eta}{\Gamma(\rho)} K \int_0^t (t - \varsigma)^{\rho} \varsigma^{\eta-1} d\varsigma, \end{aligned} \tag{6.7}$$

where,

$$K = \|\mathcal{H}\|_\infty,$$

and the norm is defined by

$$\|\chi\|_\infty = sup_{t \in \prod_a^b} \|\chi(t)\|.$$

Further, letting $\varsigma = ty$, the above expression is converted to

$$\|\Lambda\phi(t) - p(0)\| \leq \frac{\eta K}{\Gamma(\rho)} t^{\rho+\eta-1} B(\rho, \eta), \tag{6.8}$$

$$\|\Lambda\phi(t) - p(0)\| < c \Longrightarrow K < \frac{c\Gamma(\rho)}{\eta a^{\eta+\rho-1} B(\eta, \rho)}. \tag{6.9}$$

Taking $\phi_1, \phi_2 \in C[I_n(t_n), A_b(t_n)]$, we obtained the following result,

$$\begin{aligned} \|\Lambda\phi_1 - \Lambda\phi_2\| &\leq \Big(\frac{\eta L}{\Gamma(\rho)} t^{\eta+\rho-1} B(\rho, \eta)\Big) \|\phi_1 - \phi_2\| \\ &< \Big(\frac{\eta L}{\Gamma(\rho)} a^{\eta+\rho-1} B(\rho, \eta)\Big) \|\phi_1 - \phi_2\|. \end{aligned} \tag{6.10}$$

Thus, we deduce that the contractive property is arrived after the fulfilment of following criteria

$$L < \frac{\Gamma(\rho)}{\eta a^{\eta+\rho-1} B(\rho, \eta)}. \tag{6.11}$$

Hence, complete the proof.

6.2. Numerical scheme for fractal-fractional MPX model

This section briefly presents a novel numerical scheme for the fractal-fractional MPX transmission model (6.1) in order to obtain the impact of fractional and fractal orders graphically. The procedure presented in [21] is utilized for this purpose. The model presented in (6.1) is firstly converted to Volterra form as the fractional integral operator is differentiable. Further, the fractal-fractional Caputo model in the form of RL operator can be expressed as:

$$\frac{1}{\Gamma(1-\rho)}\frac{d}{dt}\int_0^t (t-\varsigma)^{-\rho} f(\varsigma)d\varsigma \frac{1}{\eta t^{\eta-1}}. \tag{6.12}$$

Therefore, the problem (6.2) can be transform as

$$^{RL}D^{\rho}_{0,t}\Big(p(t)\Big) = \eta t^{\eta-1}\Big[\mathcal{H}(t,p(t))\Big]. \tag{6.13}$$

Further, the RL derivative is replaced with the Caputo derivative such that to make the use of the integer-order initial conditions. The Eq (6.13) gives the following expression:

$$p(t) = p(0) + \frac{\eta}{\Gamma(\rho)}\int_0^t \varsigma^{\eta-1}(t-\varsigma)^{\rho-1}\mathcal{H}(\varsigma,p(\varsigma))d\varsigma. \tag{6.14}$$

Upon the grid points $t = t_{n+1}$, (6.14) can be written as follows:

$$\begin{aligned} p^{n+1} &= p_0 + \frac{\eta}{\Gamma(\rho)}\int_0^{t_{n+1}} \varsigma^{\eta-1}(t_{n+1}-\varsigma)^{\rho-1}\mathcal{H}(\varsigma,p(\varsigma))d\varsigma, \\ &= p_0 + \frac{\eta}{\Gamma(\rho)}\sum_{v=0}^{n}\int_{t_v}^{t_{v+1}} \varsigma^{\eta-1}(t_{n+1}-\varsigma)^{\rho-1}\mathcal{H}(\varsigma,p(\varsigma))d\varsigma. \end{aligned} \tag{6.15}$$

Moreover, utilizing the Lagrangian piece-wise interpolation procedure over the finite interval $[t_v, t_{v+1}]$ for the function $\mathcal{H}(\varsigma, p(\varsigma))$ in (6.15) we have

$$\mathcal{H}(\varsigma,p(\varsigma)) \approx P_v(\varsigma) = \frac{\varsigma - t_{v-1}}{t_v - t_{v-1}} t_v^{\eta-1}\mathcal{H}(t_v,p(t_v)) - \frac{\varsigma - t_v}{t_v - t_{v-1}} t_{v-1}^{\eta-1}\mathcal{H}(t_{v-1},p(t_{v-1})). \tag{6.16}$$

Using the approximation made in (6.16), the (6.15) leads to the following:

$$p^{n+1} = p_0 + \frac{\eta}{\Gamma(\rho)}\sum_{v=0}^{n}\int_{t_v}^{t_{v+1}} \lambda^{\eta-1}(t_{n+1}-\varsigma)^{\rho-1}P_v(\varsigma)d\varsigma. \tag{6.17}$$

Finally, the solution of (6.17) leads to the following equation:

$$\begin{aligned} p^{n+1} = p^0 + \frac{\eta \mathfrak{h}^{\rho}}{\Gamma(\rho+2)}\sum_{v=0}^{n}\Big[& t_v^{\eta-1}\mathcal{H}(t_v,g(t_v)) \\ & \times\Big((n+1-v)^{\rho}(n-v+2+\rho) - (n-v)^{\rho}(n-v+2+2\rho)\Big) \\ & - t_{v-1}^{\eta-1}\mathcal{H}(t_{v-1},g(t_{v-1})) \times \Big((n+1-v)^{\rho+1} - (n-v)^{\rho}(n+1-v+\rho)\Big)\Big]. \end{aligned} \tag{6.18}$$

Thus, implementing the scheme derived in (6.18) on the proposed fractal-fractal MPX transmission model (6.1), the following recursive formulae are established:

$$
\begin{aligned}
S_h^{n+1} &= S_h^0 + \frac{\eta \mathfrak{h}^\rho}{\Gamma(\rho+2)} \sum_{v=0}^{n} \Big[t_v^{\eta-1} \mathcal{H}_1(t_v, p(t_v)) \\
&\quad \times \Big((n+1-v)^\rho (n+2-v+\rho) - (n-v)^\rho (n+2-v+2\rho) \Big) \\
&\quad - t_{v-1}^{\eta-1} \mathcal{H}_1(t_{v-1}, p(t_{v-1})) \times \Big((n+1-v)^{\rho+1} - (n-v)^\rho (n+1-v+\rho) \Big) \Big], \\
I_h^{n+1} &= I_h^0 + \frac{\eta \mathfrak{h}^\rho}{\Gamma(\rho+2)} \sum_{v=0}^{n} \Big[t_v^{\eta-1} \mathcal{H}_2(t_v, g(t_v)) \\
&\quad \times \Big((n+1-v)^\rho (n+2-v+\rho) - (n-v)^\rho (n-v+2+2\rho) \Big) \\
&\quad - t_{v-1}^{\eta-1} \mathcal{H}_2(t_{v-1}, p(t_{v-1})) \times \Big((n+1-v)^{\rho+1} - (n-v)^\rho (n+1-v+\rho) \Big) \Big], \\
Q_h^{n+1} &= Q_h^0 + \frac{\eta \mathfrak{h}^\rho}{\Gamma(\rho+2)} \sum_{v=0}^{n} \Big[t_v^{\eta-1} \mathcal{H}_3(t_v, g(t_v)) \\
&\quad \times \Big((n+1-v)^\rho (n+2-v+\rho) - (n-v)^\rho (n+2-v+2\rho) \Big) \\
&\quad - t_{v-1}^{\eta-1} \mathcal{H}_3(t_{v-1}, p(t_{v-1})) \times \Big((n+1-v)^{\rho+1} - (n-v)^\rho (n+1-v+\rho) \Big) \Big], \\
R_h^{n+1} &= R_h^0 + \frac{\eta \mathfrak{h}^\rho}{\Gamma(\rho+2)} \sum_{v=0}^{n} \Big[t_v^{\eta-1} \mathcal{H}_4(t_v, g(t_v)) \\
&\quad \times \Big((n+1-v)^\rho (n+2-v+\rho) - (n-v)^\rho (n+2-v+2\rho) \Big) \\
&\quad - t_{v-1}^{\eta-1} \mathcal{H}_4(t_{v-1}, p(t_{v-1})) \times \Big((n+1-v)^{\rho+1} - (n-v)^\rho (n+1-v+\rho) \Big) \Big], \\
S_m^{n+1} &= S_m^0 + \frac{\eta \mathfrak{h}^\rho}{\Gamma(\rho+2)} \sum_{v=0}^{n} \Big[t_v^{\eta-1} \mathcal{H}_5(t_v, g(t_v)) \\
&\quad \times \Big((n+1-v)^\rho (n+2-v+\rho) - (n-v)^\rho (n+2-v+2\rho) \Big) \\
&\quad - t_{v-1}^{\eta-1} \mathcal{H}_5(t_{v-1}, p(t_{v-1})) \times \Big((n+1-v)^{\rho+1} - (n-v)^\rho (n+1-v+\rho) \Big) \Big], \\
I_m^{n+1} &= I_m^0 + \frac{\eta \mathfrak{h}^\rho}{\Gamma(\rho+2)} \sum_{v=0}^{n} \Big[t_v^{\eta-1} \mathcal{H}_6(t_v, g(t_v)) \\
&\quad \times \Big((n+1-v)^\rho (n+2-v+\rho) - (n-v)^\rho (n+2-v+2\rho) \Big) \\
&\quad - t_{v-1}^{\eta-1} \mathcal{H}_6(t_{v-1}, p(t_{v-1})) \times \Big((n+1-v)^{\rho+1} - (n-v)^\rho (n+1-v+\rho) \Big) \Big].
\end{aligned} \tag{6.19}
$$

6.3. Simulation of the fractal-fractional MPX model

The MPX transmission model (6.1) is simulated using the iterative scheme established in (6.19). The values of parameters and initial conditions are the same as considered in the fractional model. The model is simulated for three cases, considering different values of fractal order η and fractional order ρ. Model simulations are analyzed numerically in Figures 3–5. In each figure, we present the impact of the fractional and fractal orders ρ and η respectively on the solution of the model.

Case 1: In this case, the fractal order η is fixed and the fractional order ρ is varied by taking four different values, i.e., 1, 0.95, 0.90, 0.80. The simulation for this set of parameters is analyzed in Figure 3(a)–(f). The dynamics of susceptible, infected, isolated, and recovered human population classes are shown in Figure 3(a)–(d) respectively. The dynamics of susceptible and infected animal population is analyzed in Figure 3(e),(f) respectively.

Case 2: This case presents the simulation of the fractal-fractional model (6.1) when the order of the Caputo fractional operator is fixed to integer case, i.e., $\rho = 1$ and considered four different values, i.e., $\eta = 1,\ 0.9, 0.80, 0.70$ of the order of fractal operator. The simulation obtained from this scenario is depicted in Figure 4(a)–(f). The dynamics of human population classes are shown in Figure 4(a)–(d) respectively, whereas the dynamic of susceptible and infected animal compartments are respectively analyzed in Figure 4(e),(f).

Case 3: In the third case, we simulate the fractal-fractional MPX transmission model (6.1) when both the fractional order ρ and fractal order η varied equally or differently. The simulation results produced for this scenario are analyzed in Figures 5 and 6 with subplots (a)–(f). From these figures, we observed that in all three cases the solution curves converge to steady states. However, in the third case (by taking non-integer values of both ρ and η) the converges to a steady state is attained comparatively over a longer time period. Overall, we conclude that the fractal-fractional derivatives can be utilized in order to provide a better understanding of disease dynamics.

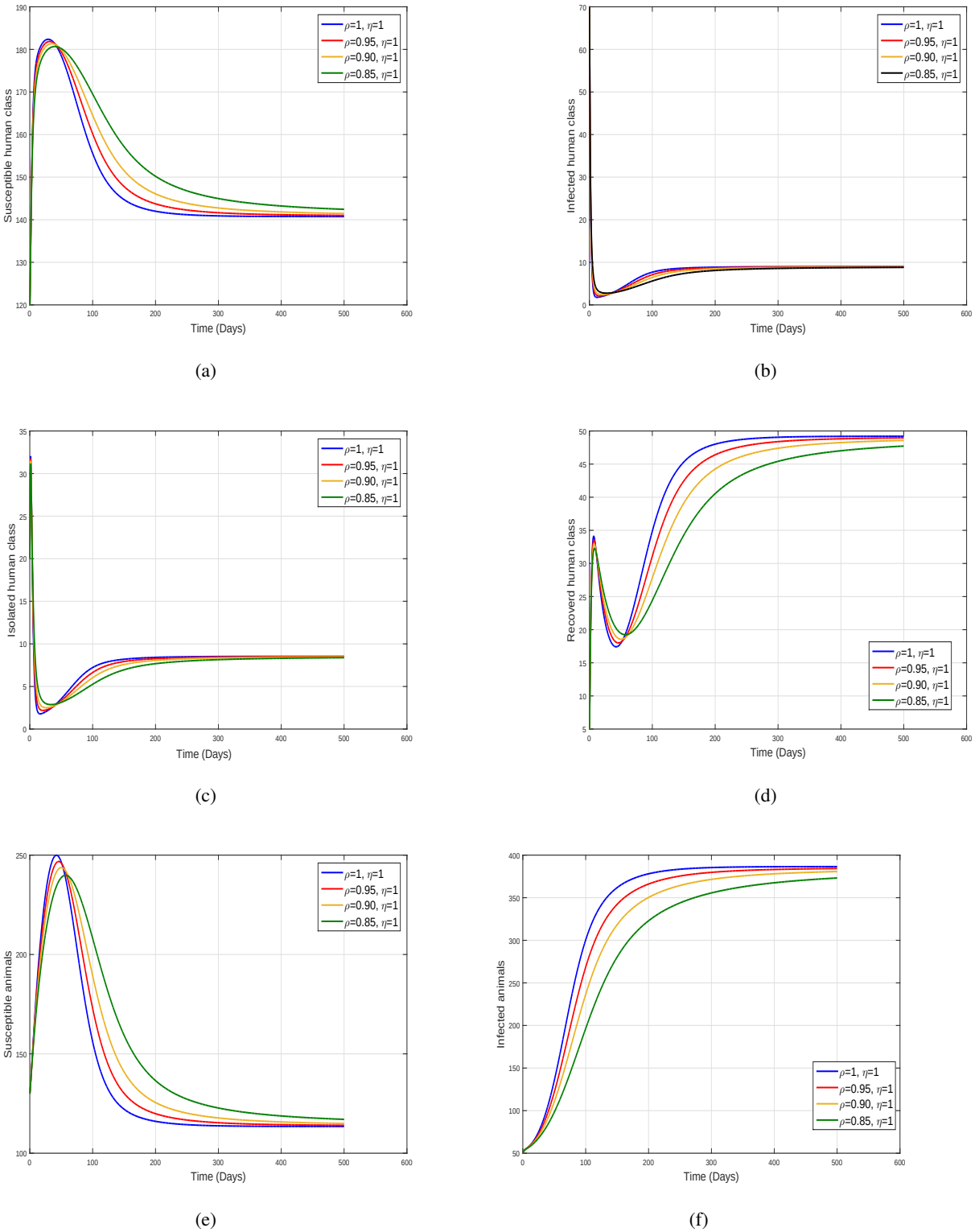

Figure 3. Case 1: Dynamics of the fractional-fractal MPX transmission model (6.1) when the fractional order is $\rho = 1, 0.95, 0.90, 0.80$ and the fractal order is $\eta = 1$.

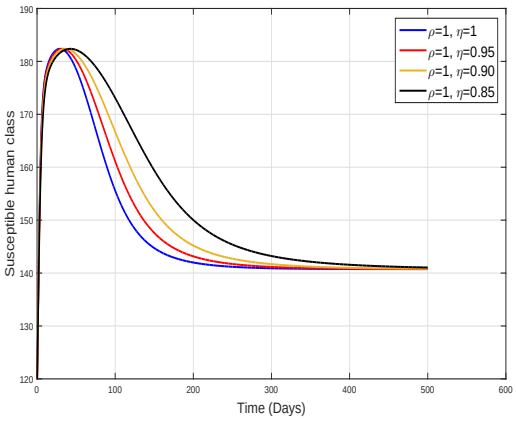

(a)

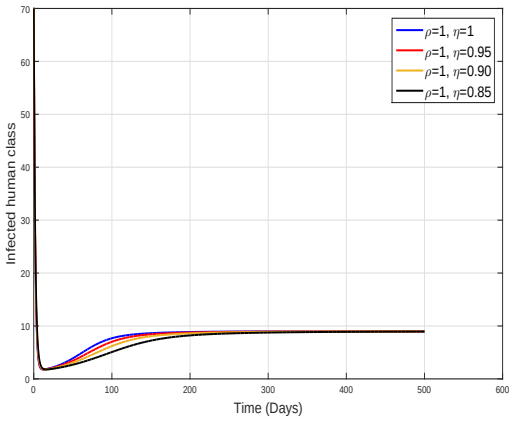

(b)

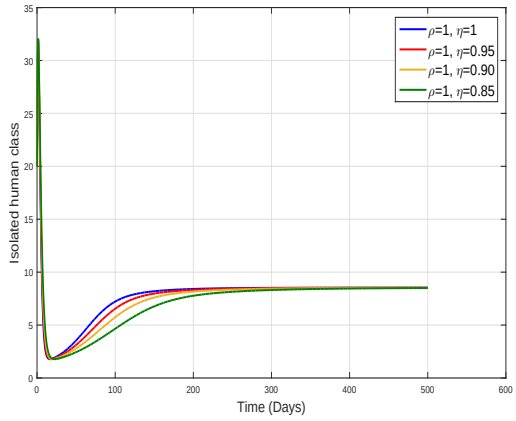

(c)

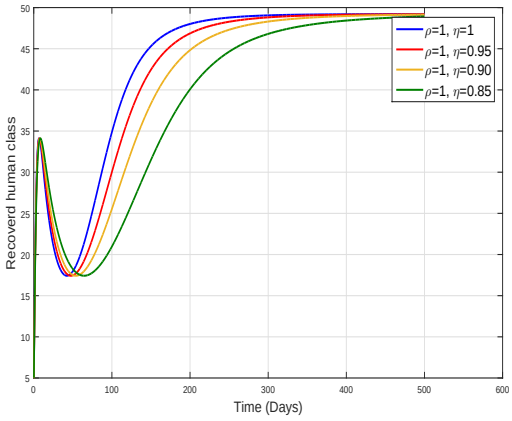

(d)

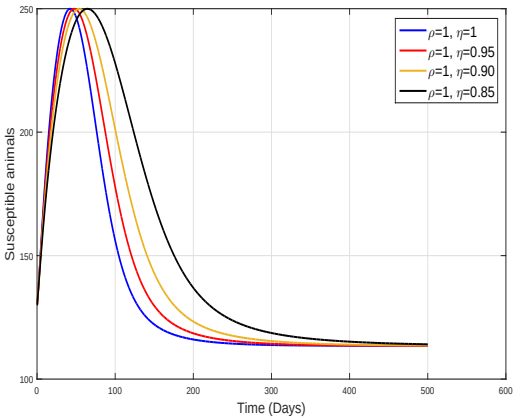

(e)

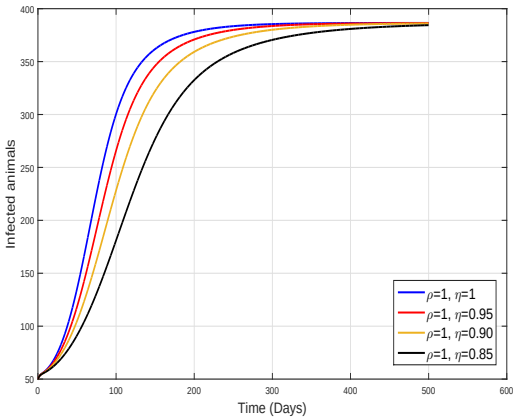

(f)

Figure 4. Case 2: Dynamics of fractional-fractal MPX model (6.1) when fractional order is $\rho = 1$ and fractal order is $\eta = 1, 0.95, 0.90, 0.80$.

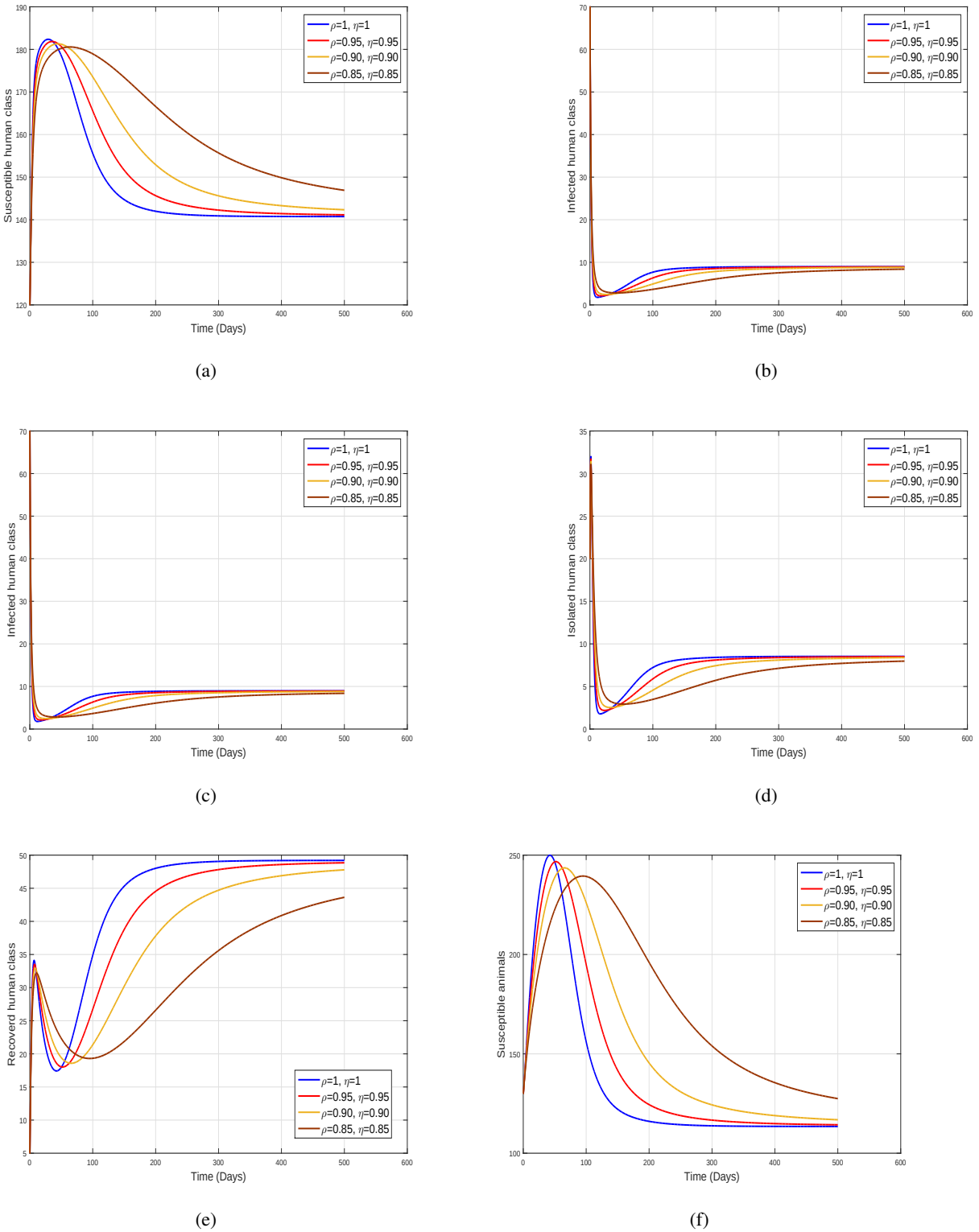

Figure 5. Case 3: Dynamics of the fractional-fractal MPX transmission model (6.1) when fractional order is $\rho = 1, 0.95, 0.90, 0.80$ and fractal order is $\eta = 1, 0.95, 0.90, 0.80$.

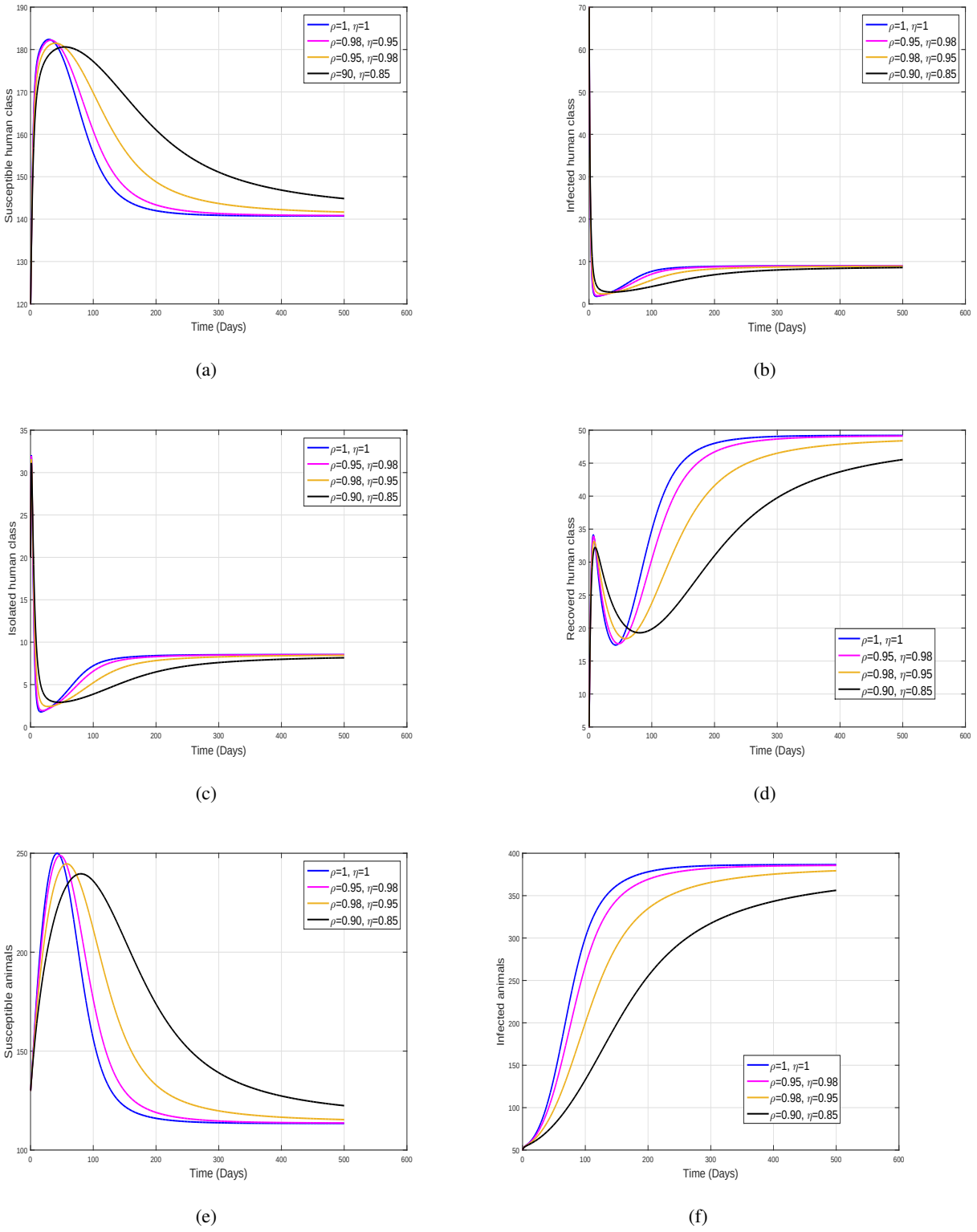

Figure 6. Simulation of the fractional-fractal MPX transmission model (6.1) when fractional order is $\rho = 1, 0.98, 0.95, 0.90$ and fractal order is $\eta = 1, 0.95, 0.98, 0.85$.

7. Conclusions

In this manuscript, a new Monkeypox epidemic model with human-to-animal transmission is analyzed. Although few cases have been reported on such transmission. To the best of over knowledge, this is the first attempt to consider such transmission in the Monkeypox transmission model. We developed the model with integer-order derivative and then extended it to fractional order via the Caputo operator to analyze the impact of memory index on the disease incidence. The basic mathematical analysis of the fractional Monkeypox model including the existence and uniqueness of the solutions is carried out in the initial stage. The fractional model is then solved numerically and the simulation is shown for two cases choosing different values of parameters demonstrating the stability of model equilibria graphically. Moreover, the model is reformulated via the novel fractal-fractional operator in order to obtain the generalized model. The existence and uniqueness of the problem solution in this case are provided via the Picard-Lindelöf approach. An efficient numerical procedure based on the Adams-Bashforth approach is used for the solution of the fractal-fractional Monkepox model. Simulation is presented for three different cases by considering various values of fractal and fractional paraments. In all cases, we observed that the solution curves converge to the model's steady state.

Acknowledgements

The authors would like to thank the Deanship of Scientific Research at Umm Al-Qura University for supporting this work by Grant Code: 22UQU4390021DSR06.

Conflict of interest

The authors declare there is no conflict of interest.

References

1. *World Health Organization*, Monkeypox, 2022. Available from: https://www.who.int/news-room/fact-sheets/detail/monkeypox.
2. *World Health Organization*, Monkeypox, 2022. Available from: https://www.who.int/news-room/questions-and-answers/item/monkeypox.
3. Centers for Disease Control and Prevention. Available from: https://www.cdc.gov/poxvirus/monkeypox/.
4. S. Ullah, M. A. Khan, M. Farooq, T. Gul, Modeling and analysis of tuberculosis (tb) in khyber pakhtunkhwa, pakistan, *Math. Comput. Simul.*, **165** (2019), 181–199. https://doi.org/10.1016/j.matcom.2019.03.012
5. A. Khan, R. Ikram, A. Din, U. W. Humphries, A. Akgul, Stochastic covid-19 seiq epidemic model with time-delay, *Results Phys.*, **30** (2021), 104775. https://doi.org/10.1016/j.rinp.2021.104775
6. X. Liu, S. Ullah, A. Alshehri, M. Altanji, Mathematical assessment of the dynamics of novel coronavirus infection with treatment: A fractional study, *Chaos, Solitons Fractals*, **153** (2021), 111534. https://doi.org/10.1016/j.chaos.2021.111534

7. S. Usman, I. I. Adamu, Modeling the transmission dynamics of the monkeypox virus infection with treatment and vaccination interventions, *J. Appl. Math. Phys.*, **5** (2017), 81078. https://doi.org/10.4236/jamp.2017.512191

8. O. J. Peter, S. Kumar, N. Kumari, F. A. Oguntolu, K. Oshinubi, R. Musa, Transmission dynamics of monkeypox virus: a mathematical modelling approach, *Model. Earth Syst. Environ.*, **8** (2022), 3423–3434. https://doi.org/10.1007/s40808-021-01313-2

9. C. P. Bhunu, S. Mushayabasa, J. Hyman, Modelling hiv/aids and monkeypox co-infection, *Appl. Math. Comput.*, **218** (2012) 9504–9518. https://doi.org/10.1016/j.amc.2012.03.042

10. A. Khan, Y. Sabbar, A. Din, Stochastic modeling of the monkeypox 2022 epidemic with cross-infection hypothesis in a highly disturbed environment, *Math. Biosci. Eng.*, **19** (2022), 13560–13581. https://doi.org/10.3934/mbe.2022633

11. I. Podlubny, *Fractional Differential Equations: An Introduction to Fractional Derivatives, Fractional Differential Equations, to Methods of Their Solution and Some of Their Applications*, Elsevier, 1998.

12. M. Caputo, M. Fabrizio, A new definition of fractional derivative without singular kernel, *Progr. Fract. Differ. Appl.*, **1** (2015), 1–13. http://dx.doi.org/10.12785/pfda/010201

13. A. Atangana, D. Baleanu, New fractional derivatives with nonlocal and non-singular kernel: theory and application to heat transfer model, *Therm. Sci.*, **20** (2016), 763–769. https://doi.org/10.2298/TSCI160111018A

14. O. J. Peter, F. A. Oguntolu, M. M. Ojo, A. O. Oyeniyi, R. Jan, I. Khan, Fractional order mathematical model of monkeypox transmission dynamics, *Phys. Scr.*, **97** (2022), 084005. https://doi.org/10.1088/1402-4896/ac7ebc

15. A. El-Mesady, A. Elsonbaty, W. Adel, On nonlinear dynamics of a fractional order monkeypox virus model, *Chaos, Solitons Fractals*, **164** (2022), 112716. https://doi.org/10.1016/j.chaos.2022.112716

16. A. Atangana, Fractal-fractional differentiation and integration: Connecting fractal calculus and fractional calculus to predict complex system, *Chaos, Solitons Fractals*, **102** (2017), 396–406. https://doi.org/10.1016/j.chaos.2017.04.027

17. W. Wang, M. Khan, Analysis and numerical simulation of fractional model of bank data with fractal-fractional Atangana-Baleanu derivative, *J. Comput. Appl. Math.*, **369** (2019), 112646. https://doi.org/10.1016/j.cam.2019.112646

18. X. P. Li, S. Ullah, H. Zahir, A. Alshehri, M. B. Riaz, B. A. Alwan, Modeling the dynamics of coronavirus with super-spreader class: A fractal-fractional approach, *Results Phys.*, **34** (2022), 105179. https://doi.org/10.1016/j.rinp.2022.105179

19. S. Qureshi, E. Bonyah, A. A. Shaikh, Classical and contemporary fractional operators for modeling diarrhea transmission dynamics under real statistical data, *Phys. A*, **535** (2019), 122496. https://doi.org/10.1016/j.physa.2019.122496

20. C. Li, F. Zeng, *Numerical Methods for Fractional Calculus*, Chapman and Hall/CRC, 2015.

21. A. Atangana, S. Qureshi, Modeling attractors of chaotic dynamical systems with fractal–fractional operators, *Chaos, Solitons Fractals*, **123** (2019), 320–337. https://doi.org/10.1016/j.chaos.2019.04.020

AIMS Press